SCA2003-48: CORE RECONSTRUCTION FROM CT SCAN POROSITY FIELDS

A. Moctezuma-Berthier[1,3], O. Vizika[1], P.M. Adler[2]
[1]Institut Français du Pétrole, BP 311, 92506-Rueil-Malmaison, France
[2]Institut de Physique du Globe de Paris, 75252-Paris, France
[3]Instituto Mexicano del Petróleo, México, D.F., México

This paper was prepared for presentation at the International Symposium of the Society of Core Analysts held in Pau, France, 21-24 September 2003

ABSTRACT

A systematic study to generate reconstructed cores using CT-scan porosity maps was conducted. The long trends, which are seen in real cores, were corrected in order to recover a stationary character. By means of an adequate transformation, the resulting porosities are transformed into Gaussian variables. Then, a correlated Gaussian field is generated to which the inverse of the previous corrections are applied. This technique was applied to two CT-scan porosity maps for two carbonates, the Brauvilliers and Estaillades samples. The methodology was more successful for the Brauvilliers sample than for the Estaillades one. The macroscopic transport properties of conductivity $\overline{s}$ and permeability $\overline{K}$ were calculated in real and reconstructed samples using the "box integration method". To generate the local conductivity and permeability fields, we used four different correlations. The results for the real and reconstructed samples are also compared with laboratory measurements. For conductivity, the comparison is very good for the Brauvilliers sample. For the Estaillades sample, the experimental value is larger than $s = s(e)$. In terms of permeability, the results show that the global permeability for Brauvilliers is not very sensitive to the correlations $K=K(e)$; for the Estaillades sample, a significant influence of the porosity correlation was observed.

CT-SCAN 3D POROSITY MAP

The X-ray attenuation is proportional to the material density, and porosity is determined by two successive measurements at water saturations S_w=0 and 1 by conventional image substraction. Fig. 4 (lower) shows one example of a longitudinal section of the porosity map obtained using this technique.

STATISTICAL ANALYSIS

Mean porosity and correlation function: The measured core porosity field $e(\mathbf{x})$ can be characterize d in a statistical sense by the two average properties

$$\bar{e} = \overline{e(\mathbf{x})} \qquad (1a) \qquad\qquad R_e(\mathbf{u}) = \frac{\lfloor e(\mathbf{x}) - \bar{e} \rfloor \cdot \lfloor e(\mathbf{x}+\mathbf{u}) - \bar{e} \rfloor}{(\bar{e} - \bar{e}^2)} \qquad (1b)$$

where $\bar{e}$ is the mean porosity value and $R_e(\mathbf{u})$ the correlation function of porosity; $\mathbf{u}$ is the translation vector and $\mathbf{x}$ denotes the position. Fig. 3 shows the correlation function for the experimental CT-scan porosity map.

The correlations show that the Brauvilliers sample is isotropic; in contrast, the Estaillades sample is orthotropic; the two axes x and y are equivalent, and different from z.

It is interesting to note that the permeability tensor is isotropic for the Estaillades sample, and anisotropic for the Brauvilliers sample (cf. Clavaud, 1996). This contradiction illustrates the difficulty to find an adequate correlation between porosity and permeability in some carbonates (Lucia, 1999; Moore, 2002; Clavaud, 1996).

Corrections for long trends: Long porosity trends can be present in real samples. They can be obtained by averaging porosity in cross sections perpendicular to the direction under study. Hence, one can introduce the three following variables

$$E_i(x_i) = \frac{1}{S_i} \iint_{S_i(x_i)} e(\mathbf{x}) dx_j dx_k \qquad i=1,2,3;\ j \neq k \neq i \qquad (2)$$

where $S_i(x_i)$ is the cross section of the sample perpendicular to the j and k axes; $S_i(x_i)$ is characterized by the value of the coordinate x_i. The porosity trend along the core was corrected from the direct porosity data by $e'(x,y,z) = e(x,y,z) - a_1 x_1 - a_2 x_2 - a_3 x_3 - B$ where $B = b_1 + b_2 + b_3 + \langle e \rangle$ (a_i and b_i are the linear regression coefficients).

Correction for non-Gaussian distributions: When the long trends are removed from the porosity variations, the probability density of the fluctuations e' can be analyzed and compared to a Gaussian density with the same average and the same variance. This comparison is displayed in Fig. 1.

To make a change of variables $g=T(e')$ where the random variable g is Gaussian, let $G(y)$ be the distribution function of a Gaussian variable y; hence,

$$G(y) = \frac{1}{\sqrt{2\pi\sigma}} \int_{-\infty}^{y} e^{-\frac{(r-\mu)^2}{2\sigma^2}} dr \qquad (3)$$

The distribution function of the porosity fluctuation is defined by $F(e'_0) = \mathrm{Prob}\{e' \leq e'_0\}$. The variable g is assumed to be Gaussian; thus, $\mathrm{Prob}\{g \leq g_0\} = G(g_0)$. The first relation can be expressed as $F(e'_0) = \mathrm{Prob}\{e' \leq e'_0\} = \mathrm{Prob}\{g \leq T(e'_0)\} = G[T(e'_0)]$. Since $G(y)$ is an increasing monotonic function, it can be inverted and one obtains $T(e'_0) = G^{-1}\left[F(e'_0)\right]$. In that way the correspondence function T can be derived from the experimental data.

Correlation functions for the field $g(\mathbf{x})$: It is important to note that the correlation functions $R_e(\mathbf{u})$ are modified by the two previous changes of variables $e \rightarrow e' \rightarrow g$. Let m_g and s_g be the mean and the standard deviation of the field g.

The correlation function $R_g(\mathbf{u})$ can be defined exactly as $R_e(\mathbf{u})$ (cf. (1b)) by replacing e by g. It can be directly computed on the sample. Results are displayed in Fig. 2.

RECONSTRUCTION

Generation of a random correlated field: The generation is based on the method developed by Adler et al (1990) that generates a random and stationary population $Y(\mathbf{r})$ with a given spatial correlation $R_Y(\mathbf{u})$ by using the Fourier transform technique.

Since the generated correlated random field $Y(\mathbf{x})$ has a standard normal distribution (with a zero mean and variance equal to one), it is then restored in terms of the mean m_g and the standard deviation s_g by $g_R(\mathbf{x}) = Y(\mathbf{x})s_g + m_g$. The inverse of the transformation $T^{-1}(\mathbf{x})$ and the inversion of the porosity trends are applied to the field $g_R(\mathbf{x})$ in order to have the reconstructed porosity map $e_R(\mathbf{x})$ in the same terms as the original experimental CT field $e(\mathbf{x})$.

The correlation function $R_{e_R}(\mathbf{u})$ of the reconstructed field $e_R(\mathbf{x})$ is compared to the original experimental correlation function $R_e(\mathbf{u})$; these results are presented in Fig. 3 for both samples. We can see that for the Brauvilliers sample the correlation function of the reconstruction sample is in very good agreement with the experimental correlations. For the Estaillades sample, the reconstruction reproduces the anisotropy, but does not agree with the original experimental data. In Fig. 4, we display (lower) an original core section and a reconstructed one (upper) obtained for the Brauvilliers sample; we can see that the visual comparison is satisfactory.

MACROSCOPIC PROPERTIES

The macroscopic conductivity $\overline{s}$ and permeability $\overline{K}$ were calculated for the original CT-scan porosity map in both samples and in the Brauvilliers reconstruction. These properties are obtained by solving the conservation equation on the Darcy scale.

Conductivity: The conductivity is given by the master curve of Moctezuma-Berthier et al (2002) by

$$s(e) = 1.2483e^2 - 0.2599e + 0.0116 \qquad (4)$$

corresponding to a homogeneous system with a Gaussian correlation function $R_Y(\mathrm{u})$ on pore scale. Fig. 5 shows the conductivity calculations. For the Brauvilliers sample, it is interesting to note that the results for the reconstructed sample follow (4); moreover, the calculations are in very good agreement with the measured values. For the Estaillades sample, we can see that the measurement is not so close to (4), but the calculations for the experimental field $e(\mathbf{x})$ compare well with (4).

Permeability: Moctezuma-Berthier et al (2003) presented two models that fit the local permeability of vugular porous media with a Gaussian correlation function $R_Y(u)$ on pore scale. The experimental values for permeability are set by using the size of the elementary cubes (a[µm], used for the numerical discretizations) as a fitting parameter. The dimensionless expression for a vuggy system can be written as

$$K / l_v^2 = K*_H(e_t) - \left[K*_H(e_t) - K*_H(e_v)\right] \cdot \left[1 - 1.2(l_p / l_v)^2\right] \quad (5)$$

where $K*_H$ corresponds to a unimodal medium $K*_H(e) = K_H / l_v^2 = 0.0295 e^{4.1854}$; e_t and e_v are the total and vug porosities. l_p and l_v are the characteristic lengths of the pores and of the vugs. Three different cases were studied; one considered the correlation for a unimodal porous medium with $e_t = e_v$; the two others are bimodal media with $e_v = 0.15$ and $l_v/l_p = 2$ and 4. For the Brauvilliers sample (Fig. 6a), we can see that the calculations have a maximum of 9% for the unimodal case using the $e(x)$ field. When using the reconstructed porosity map $e_R(x)$, the sensitivity to (5) is smaller; the permeability values calculated for the three different cases are of the same order of magnitude and close to (5). For the Estaillades sample (Fig. 6b), the maximum variation is 10% when (5) and the $e(x)$ field are used for the unimodal case; the sensitivity to (5) is greater than for the Brauvilliers sample and when higher ratios l_v/l_p are used, results are closer to (5).

CONCLUDING REMARKS

Experimental porosity maps from CT scan data were used for porosity reconstruction with the same statistical characteristics. The methodology was more successful for the Brauvilliers sample than for the Estaillades ones; this is possibly due to the more complex porosity distribution of the second one.

Comparison of macroscopic calculations with experimental results for conductivity shows a good agreement both for the experimental CT field and for the reconstructed field for the Brauvilliers sample. For the Estaillades sample, the experimental value is larger than (4), but the calculation using the original CT porosity field was consistent with (4).

The numerical results show that the global permeability for Brauvilliers is not very sensitive to the different cases of (5). For the Estaillades sample, calculations using the CT porosity field showed a high influence of (5); when the ratio l_v/l_p increases, $\overline{K}$ tends towards (5).

REFERENCES

1. Adler P.M., 1992. *Porous Media, Geometry and Transports*, Butterworth-Heinemann.
2. Adler P.M., Jacquin C.G. and Quiblier J. A., 1990. *Flow in Simulated Porous Media*, Int. J. Multiphase Flow, **16**, 691-712.
3. Clavaud J. B., 1996. *Etude Expérimentale et Numérique de l'anisotropie de Perméabilité des Roches Poreuses par Tomographie-X.* Technical Report of a stay at the Institut Français du Pétrole. France.

4. Lucia, F. J., 1999. *Carbonate Reservoir Characterization* , Springer.
5. Moctezuma-Berthier A., Vizika O. and Adler P.M., 2002. *Macroscopic Conductivity of Vugular Porous Media*. Transport in Porous Media, **49**, 313-332.
6. Moctezuma-Berthier A., Vizika O. and Adler P.M., 2003. *One and Two Phase Permeabilities of Vugular Porous Media*. In Submission.

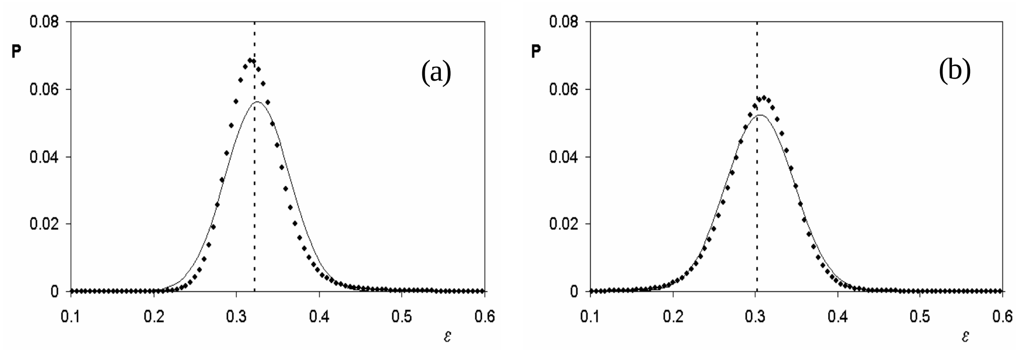

Fig 1. Probability density for the experimental field ε(x) represented by dots. (a) correspond to the Brauvilliers sample and (b) to the Estaillades sample. The dotted lines represent the mean value, and the continuous lines the Gaussian statistics, respectively.

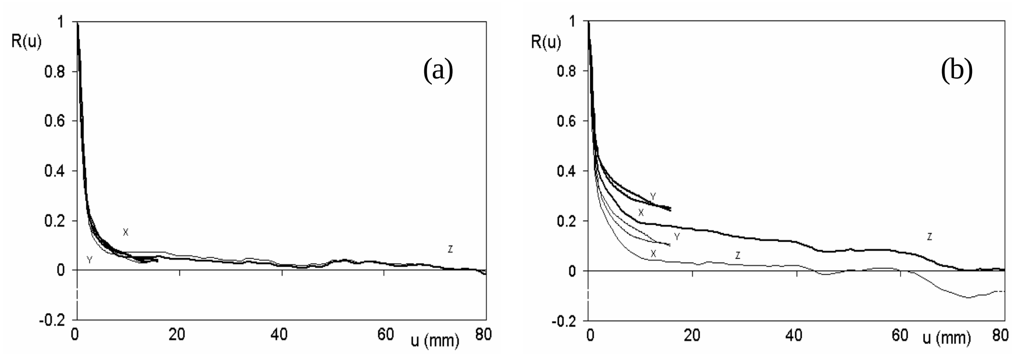

Fig. 2.- Comparison between the original correlation function R_ε(u) (thick lines) for the porosity map ε and for the "corrected" map. γ is represented by the thin lines. (a) Brauvilliers sample, (b) Estaillades sample.

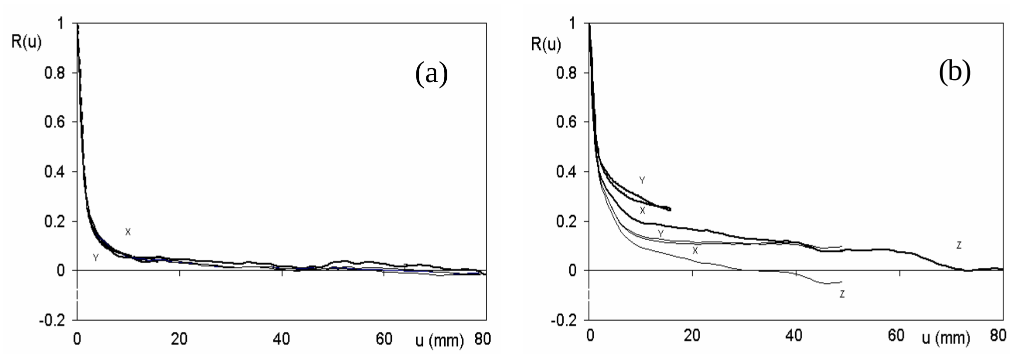

Fig. 3.- Comparison between correlation functions. The dark lines correspond to the porosity reconstructed field $R_{e_R}(\mathbf{u})$ and the thin lines to the original CT porosity map R_e(u). (a) Brauvilliers sample and (b) Estaillades sample.

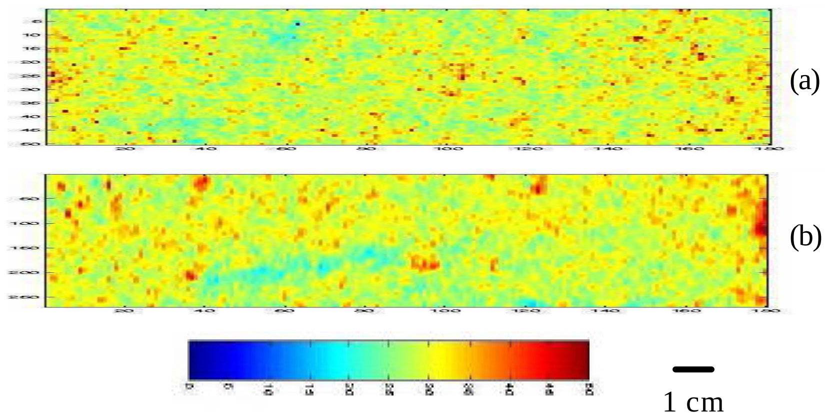

Fig. 4.- Sections of the Brauvilliers sample. (a) corresponds to the reconstructed porosity field e_R(x). (b) corresponds to the experimental CT porosity map e(x).

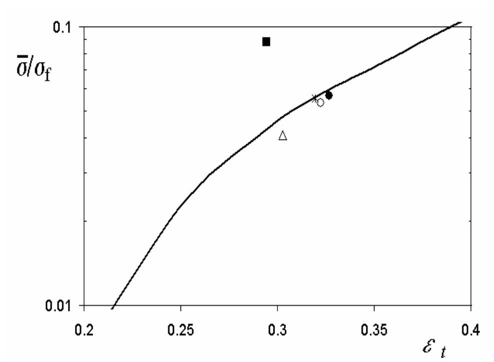

Fig. 5.- Macrosocopic conductivity $\bar{s}/s_f$ values for the experimental and reconstructed samples. The laboratory measurements are represented by the full symbols (?) for Brauvilliers and (¦) for Estaillades samples. The other symbols correspond to: Brauvilliers sample with the field e(x) (?) and with the field e_R(x) (*); Estaillades sample with the field e(x) (?). The solid line represents (4).

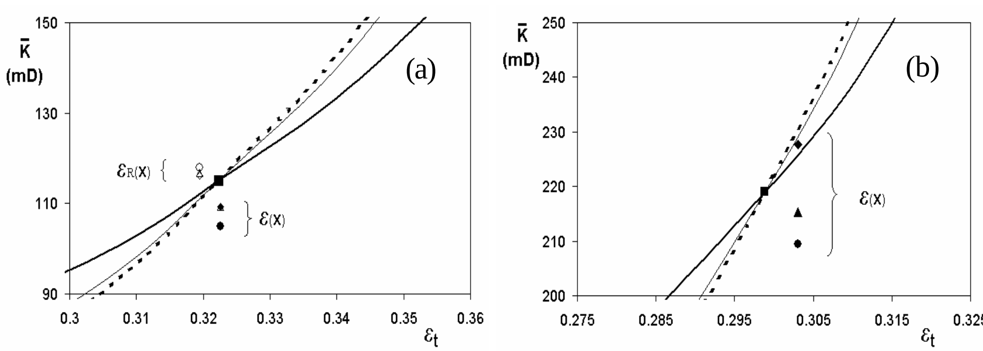

Fig. 6.- Permeability correlation for the stochastic simulations at pore scale with a Gaussian distribution R_Y(u) (Moctezuma et al., in press) and permeability results. (a) Brauvilliers and (b) Estaillades samples. Black square symbols correspond to the experimental measurements; Brauvilliers: $\overline{K}_{exp}$ =115mD, $\overline{e}_{exp}$ =0.324 . Estaillades: $\overline{K}_{exp}$ =219mD, $\overline{e}_{exp}$ =0.299. The lines represent

(5); the dotted line is for the unimodal case with e_t=e_v ; the thin and dark lines are for the bimodal cases with l_v/l_p=2 and l_v/l_p=4, respectively; in all cases l_p=6a. For the bimodal cases e_v=0.15. Black symbols correspond to the calculations performed using the e(x) porosity field; hollow symbols correspond to the reconstructed e_R(x) field (Brauvilliers sample). Data are for: unimodal (?); bimodal (? for l_v/l_p=2), (? for l_v/l_p=4).